

Gutenberg-Richter and characteristic earthquake behavior in simple mean-field models of heterogeneous faults

Karin Dahmen and Deniz Ertaş*

Lyman Laboratory of Physics, Harvard University, Cambridge, Massachusetts 02138

Yehuda Ben-Zion

Department of Earth Sciences, University of Southern California, Los Angeles, California 90089-0740

(Received 17 February 1998)

The statistics of earthquakes in a heterogeneous fault zone is studied analytically and numerically in a mean-field version of a model for a segmented fault system in a three-dimensional elastic solid. The studies focus on the interplay between the roles of disorder, dynamical effects, and driving mechanisms. A two-parameter phase diagram is found, spanned by the amplitude of dynamical weakening (or ‘‘overshoot’’) effects ϵ and the normal distance L of the driving forces from the fault. In general, small ϵ and small L are found to produce Gutenberg-Richter type power law statistics with an exponential cutoff, while large ϵ and large L lead to a distribution of small events combined with characteristic system-size events. In a certain parameter regime the behavior is bistable, with transitions back and forth from one phase to the other on time scales determined by the fault size and other model parameters. The implications for realistic earthquake statistics are discussed. [S1063-651X(98)07508-4]

PACS number(s): 05.40.+j, 91.30.Px, 62.20.Mk, 68.35.Rh

I. INTRODUCTION

The statistics of earthquakes has been a subject of research for a long time. One spectacular feature is the wide range of observed earthquake sizes, spanning over ten decades in earthquake moment magnitude (which is defined to scale as the logarithm of the integral of slip along the fault during the earthquake [1]). Gutenberg and Richter [1] found in the 1950s that the size distribution of regional earthquakes follows a power law over the entire range of observed events. The exponent b of the power-law distribution appears to be universal, i.e., it is approximately the same (within statistical errors and possible secondary dependency on the tectonic domain) for all studied regions. This type of power-law distribution is called the ‘‘Gutenberg-Richter’’ distribution. Recently, enough data has been collected to extract statistics on individual systems of earthquake faults, or more precisely on systems of narrow fault zones. Interestingly, it was found that the distribution of earthquake magnitudes may vary substantially from one fault system to another. In particular, Wesnousky and co-workers [2] found that fault systems with highly irregular geometry, such as the San Jacinto fault zone in California, which have many offsets and branches, display ‘‘power-law’’ statistics over the whole range of observed magnitudes. Not all fault systems, however, display a power-law distribution on all scales up to the largest earthquakes. The available data [2] indicates that fault systems with more regular geometry (presumably generated progressively with increasing cumulative slip) such as the San Andreas fault in California display power-law distribu-

tions only for small events, which occur in the time intervals between roughly quasiperiodic earthquakes of a much larger ‘‘characteristic’’ size which rupture the entire fault. There are practically no observed earthquakes of intermediate magnitudes on such geometrically regular fault systems. Distributions of this type are called ‘‘characteristic earthquake’’ distributions.

In previous work [3,4] it was demonstrated that a class of simple models of ruptures along a heterogeneous fault zone displays both types of behavior. The universal power-law scaling behavior of earthquake statistics was seen to be due to an underlying critical point, which becomes mean-field-like for fault geometries with more than two spatial dimensions. In the limit of *weak* dynamical effects, the mean-field approximation to the two-dimensional fault provides a more appropriate approximation than, for example, traditionally studied one-dimensional approximations to the models. In fact, *exact* results for the scaling exponents (up to logarithmic corrections) could be obtained from mean-field theory. The reason is that the elastic stresses along the fault are effectively long range (decaying like the inverse cube of the distance), such that in two and higher dimensions the fluctuations due to interaction with other points on the fault decrease as the fault size is increased—on long length scales the behavior becomes the same as that of a system with infinite ranged elastic interactions (up to logarithmic corrections in two dimensions). In other words, the upper critical dimension is equal to the physical dimension of the fault, which is 2 [5,6]. (Some of the static mean-field exponents turned out to be the same as in other quasistatic models [5].) In the presence of small but nonzero weakening effects of amplitude ϵ a critical rupture size (slipping area) n_{cr} for ‘‘runaway’’ or ‘‘characteristic fault size’’ events was calculated perturbatively [4] and was found to scale as $1/\epsilon^2$. Faults of larger area than this size are expected to display the characteristic earthquake distribution, with small events up to

*Present address: Exxon Research and Engineering, Clinton Twp., Route 22 East, Annandale, New Jersey 08801. Electronic address: mdertas@erenj.com

size n_{cr} , and no events of intermediate size between n_{cr} and the characteristic fault size events. For faults of smaller total area than n_{cr} only the power-law scaling region of the small events is seen, so the distribution is of the Gutenberg-Richter type.

In this paper we examine a mean-field model with a range of dynamical weakening effects from weak to strong, and different levels of disorder in the brittle properties. Specifically, we study the model of Ben-Zion and Rice [3], which involves simple approximations of dynamic frictional weakening (similar to static versus dynamic friction), but replace the physical long range elastic interactions with infinite range interactions. In addition to exhibiting both ‘‘power-law’’ and ‘‘characteristic’’ scaling of event sizes, this model exhibits the possibility of *coexistence* of these two types of behavior. That is, for a given set of model parameters, the system has *two distinct persistent stationary states*. In an infinitely large system it will depend on the initial conditions whether the system displays Gutenberg-Richter or characteristic earthquake type behavior. Faults of *finite* size can spontaneously switch from one state to the other on time scales that are exponentially large in system size. The switching times (or ‘‘persistence times’’) are determined by nucleation processes from one state to the other, similar to flips back and forth at coexistence in finite thermally equilibrated systems. Many of the qualitative features seem to be sufficiently robust to be applicable to real fault zones. Interesting to note, such ‘‘switching’’ behavior appears to characterize long paleoseismic records observed along the Dead Sea transform fault system in Israel [7], and is compatible with other paleoseismic [8] and geologic [9] data. In addition, qualitatively similar switching has been recently found in regional models of disordered fault systems [10].

The remainder of this paper is organized as follows. In Sec. II we define the model and provide a summary of the main results. In Sec. III we present a detailed analysis of the model along with comparisons with numerical simulations. In Sec. IV we compare our results with earlier studies of similar models and discuss their potential relevance to natural fault systems modeled as a narrow fault zone in a three-dimensional elastic surrounding medium.

II. THE MODEL AND SUMMARY OF RESULTS

Ben-Zion and Rice [3] suggested that a heterogeneous fault system with offsets and branches may be represented by an array of discrete cells in a two-dimensional plane, with spatially varying ‘‘macroscopic’’ constitutive parameters that model the heterogeneity of the original fault system. This model fault on the (x, z) plane can be considered as a collection of brittle patches mapped onto the interface between two tectonic blocks, which move with (small) relative transverse velocity $v\hat{x}$ far away from the fault. In the simple realizations used in Refs. [3,4], and here (as in related models [11]), the fault plane is segmented into N geometrically equal cells. In the mean-field approximation of infinite range elastic interactions, the local stress τ_i on cell i is given by

$$\tau_i = J/N \sum_j (u_j - u_i) + K_L(vt - u_i)$$

$$= J\bar{u} + K_L vt - (K_L + J)u_i, \quad (1)$$

where u_i is the total fault offset of cell i in the horizontal (x) direction, $\bar{u} = (\sum_j u_j)/N$, J/N is the elastic coupling between cells in the mean-field approximation, and K_L is the effective loading stiffness of the bulk material surrounding the fault patch.

Initially, the fault is in a relaxed configuration, i.e., all stresses are less than a local *static* failure threshold stress $\tau_{s,i}$. In the absence of brittle failures the stresses at the cells increase uniformly due to the external loading and $\dot{\tau}_i = K_L v$. As long as no cell reaches its failure threshold, $\dot{u}_i = 0$ everywhere. When the stress at a cell becomes larger than $\tau_{s,i}$, the cell slips by an amount $\delta u_i = (\tau_{s,i} - \tau_{a,i})/(K_L + J)$, to reduce its stress from $\tau_{s,i}$ to an arrest stress $\tau_{a,i}$. (The nonuniformity of failure and arrest stresses across the fault plane models the spatial heterogeneity of real fault zones [3].) Consequently, during failure cell stresses change by [cf. Eq. (1)]

$$\delta\tau_i = \tau_{a,i} - \tau_{s,i}, \quad (2a)$$

$$\delta\tau_j = (c/N)(\tau_{s,i} - \tau_{a,i}), \quad j \neq i \quad (2b)$$

where $c \equiv J/(K_L + J)$ is a ‘‘conservation parameter’’ giving the fraction of the stress drop of the failing cell retained in the system after the slip. As pointed out in Refs. [4,12], for fault zones with characteristic linear dimensions of $O(L)$, the ‘‘loading spring constant’’ is $K_L \sim 1/L$, provided that the stress loading of the fault is either due to uniformly moving (creeping) boundaries or applied forces at distances of $O(L)$ away from the fault plane. For the case $N = L^2$, $(1 - c) \sim O(1/\sqrt{N})$. A value $c < 1$ for a large system would be physically realized if the external drive is closer to the fault than its linear extent.

During the failure process, the slipped cell is assumed to be weakened by the rupture, such that its failure strength is reduced to a *dynamical* value $\tau_{d,i} \equiv \tau_{s,i} - \epsilon(\tau_{s,i} - \tau_{a,i})$, with $0 \leq \epsilon \leq 1$ parametrizing the relative importance of dynamical weakening effects in the system. If the failure stress transfer brings other cells to their failure threshold, an avalanche of cell failures, i.e., ‘‘rupture propagation,’’ occurs according to Eqs. (2) until all cells are at stresses $\tau_i \leq \tau_{s,i}$ [13]. It is assumed that these avalanches happen on time scales short compared to the external loading time (i.e., v is adiabatically small), so that the external load is kept constant during an earthquake. In time intervals between earthquakes, all cells are assumed to heal completely, thus failure thresholds are reset to their static value $\tau_{s,i}$ and the external loading resumes until the next cell failure.

In order to simplify notation, it is useful to introduce rescaled stress variables

$$s_i \equiv 1 - \frac{\tau_{s,i} - \tau_i}{\langle \tau_{s,i} - \tau_{a,i} \rangle}, \quad (3)$$

$$s_{a,i} \equiv 1 - \frac{\tau_{s,i} - \tau_{a,i}}{\langle \tau_{s,i} - \tau_{a,i} \rangle}, \quad (4)$$

$$s_{d,i} \equiv 1 - \frac{\tau_{s,i} - \tau_{d,i}}{\langle \tau_{s,i} - \tau_{a,i} \rangle} = 1 - \epsilon(1 - s_{a,i}), \quad (5)$$

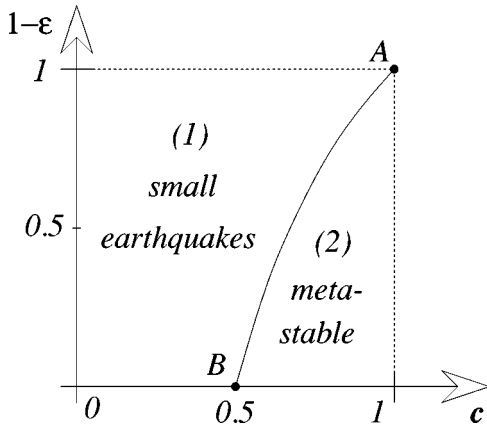


FIG. 1. Schematic phase diagram of the system. There is a “co-existence” of two persistent stationary states called Gutenberg-Richter and runaway phases, in a finite region of parameter space, marked region “(2) metastable.” For region 1 given by $c < c^* = 1/(1 + \epsilon)$ (line AB) one finds only small avalanches, i.e., the system is always in the Gutenberg-Richter phase.

such that cell failure always occurs when $s_i = 1$, and $\langle s_a \rangle = 0$. (Here, $\langle \rangle$ symbolizes averaging over all cells in the fault zone.) The arrest stress $s_{a,i}$ is uncorrelated from cell to cell, and is picked once for each segment from a probability distribution $\rho(s_a)$ with mean 0 and a compact support $(-W/2, W/2)$ of width $0 \leq W \leq 2$, which characterizes the heterogeneity of the fault system. [In our simulations we have used the parabolic distribution $\rho(s_a) = 3(W^2 - 4s_a^2)/(2W^3)$, for $-W/2 \leq s_a \leq W/2$ and 0 otherwise.] Unless stated otherwise, the focus is on the small disorder limit $W \ll 1$ and moderate values for ϵ , which are considered fixed, and the properties of the system are analyzed as a function of varying conservation parameter c and system size N . (In the last section of the paper we discuss the effects of larger values of W as well.) The size of an earthquake refers to the number of cells that failed (i.e., the “area” on the fault that slips in an earthquake).

For $N \rightarrow \infty$, depending on relative values of the system parameters, there are in general two possible steady-state distributions of cell stresses and of earthquake magnitudes. We refer to these as “phases.”

(A) The “Gutenberg-Richter” (GR) phase. This phase, possible in both regions 1 and 2 of Fig. 1, is characterized by a distribution of earthquake sizes $p_e^{(f)}(n)$ of power-law form. In infinite systems ($N \rightarrow \infty$), it is given by

$$p_e^{(f)}(n) \approx A_f n^{-3/2} \exp(-n/n_{cf}), \quad n \ll N \quad (6)$$

with a characteristic cutoff size $n_{cf} \approx 2(1-c)^{-2}$ that diverges as $c \nearrow 1$. [Finite-size corrections are given in Eq. (15) below]. The stress s_i at a given cell is independent of all others and is equally likely to take any allowable value, i.e.,

$$\text{Prob}(s \leq s_i \leq s + ds) = \frac{ds}{1 - s_{a,i}}, \quad s_{a,i} \leq s \leq 1. \quad (7)$$

Thus the stress distribution in the GR phase is given by

$$p^{(f)}(s) = \int_{-\infty}^s ds_a \frac{\rho(s_a)}{1 - s_a}, \quad (8)$$

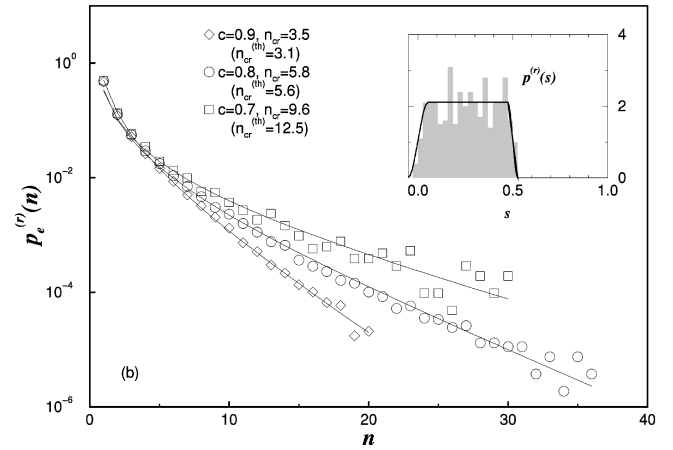
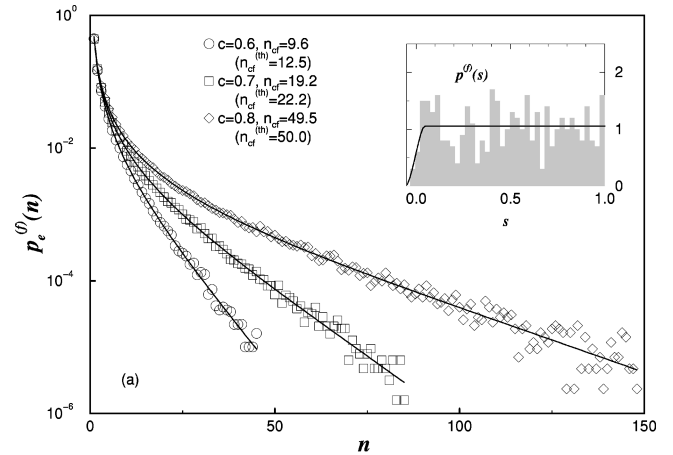


FIG. 2. Histograms of event size distributions in the two stationary states (phases), for $W = 2/19$, $\epsilon = 0.5$, $N = 400$. (a) The “Gutenberg-Richter” phase, characterized by a power-law earthquake distribution with an exponential cutoff. Solid lines are fits to the analytic form (15) with n_{cf} as a fitting parameter. Also indicated are analytic estimates $n_{cf}^{(th)}$. The inset shows a typical stress distribution of this phase for $c = 0.7$. The solid line is a fit to the analytic form (8). The nonuniform region near $s = 0$ extends from $-W/2$ to $W/2$. (b) The “runaway” phase, with a similar background distribution and large characteristic events. The inset shows a typical stress distribution for $c = 0.8$. The solid line is a fit to the analytic form (10). The nonuniform region near $s = 0$ extends from $-W/2$ to $W/2$. Near $s = \epsilon$ it extends from $\epsilon(1 - W/2)$ to $\epsilon(1 + W/2)$.

which is uniform and equal to $\bar{p} \equiv \langle (1 - s_a)^{-1} \rangle$ in the interval $(W/2) \leq s \leq 1$ [see Fig. 2(a), inset]. In this phase each cell fails at most once during an earthquake, and therefore dynamical effects are largely irrelevant. An infinitely large system which started in the GR phase will remain in this phase. In finite systems $N < \infty$, with parameters in region 2 of Fig. 1, however, a very large earthquake of size $(1 - \epsilon)N/c$ or greater occasionally triggers dynamical effects that lead to a catastrophic “runaway” event in which all cells eventually fail and cause a substantial change in the stress distribution and subsequent evolution of the system, as outlined next.

(B) The “runaway” phase. This phase is characterized by a quasiperiodic occurrence of system wide earthquakes in which all cells fail. As a result of dynamical effects, the stress s_i in a cell immediately after such a “runaway” event is independent of other cells and is equally likely to take any

value between its arrest stress and dynamical failure stress, i.e.,

$$\text{Prob}(s \leq s_i \leq s + ds) = \frac{ds}{s_{d,i} - s_{a,i}}, \quad s_{a,i} \leq s_i \leq s_{d,i}. \quad (9)$$

The stress distribution is thus given by

$$p^{(r)}(s) = \frac{1}{1 - \epsilon} \int_{[s - (1 - \epsilon)]/\epsilon}^s ds_a \frac{\rho(s_a)}{1 - s_a}, \quad (10)$$

which is uniform and equal to $\bar{p}/(1 - \epsilon)$ in the interval $(W/2) \leq s \leq 1 - \epsilon - (\epsilon W/2)$ [see Fig. 2(b), inset]. The runaway event is followed by a quiescent period during which stresses on the cells build back up from their dynamic failure value to near their static failure value. Subsequent small events are followed by the next runaway event, at which point the stress distribution is reset to Eq. (10). These background small events have a size distribution similar to events in the GR phase, but with a different cutoff size. In an infinite system [for finite-size corrections see Eq. (18) below]:

$$p_e^{(r)}(n) \approx A_r n^{-3/2} \exp(-n/n_{cr}), \quad n \ll N \quad (11)$$

$$n_{cr} \approx \frac{2(1 - \epsilon)^2}{(1 - \epsilon - c)^2}, \quad (12)$$

which diverges as $c \searrow (1 - \epsilon)$. However, this divergence is never observed, as the runaway phase becomes unstable against breakup into the GR phase when $c < c^* \equiv (1 + \epsilon)^{-1}$ for the following reason: If the background small events during a cycle involve at least a fraction r_c of the cells, the subsequent large event is unable to cause all of the cells to fail, since the cells that failed during background activity are farther away from their failure stress. This typically causes a spontaneous breakup of the bunched stress distribution and a resumption of the GR phase. The fraction of cells needed to cause this breakup is given by $r_c = 1 + \epsilon - c^{-1} = (c^*)^{-1} - c^{-1}$ as is derived in Sec. III. When $c \searrow c^*$, the size of background events necessary to cause breakup vanishes and the runaway phase becomes unstable, i.e., for $c < c^*$ the GR phase is the only persistent phase, regardless of the initial conditions. For $c > c^*$, the GR phase and the runaway phase are both persistent in an infinite system. In an infinite system the initial conditions determine which one the system displays. In a finite system, however, exponentially rare earthquakes can lead to nucleation from the GR phase into the runaway phase and vice versa. Equations (16) and (20) below give estimates of the times spent in the respective phases between such nucleation (or ‘‘switching’’) events.

III. ANALYSIS OF THE MODEL

The results quoted above have been obtained by mapping earthquakes in the model to corresponding events in a stochastic process, which is approximated by a series of Bernoulli trials [14] in order to be able to obtain analytical estimates for the various quantities of interest, such as distributions of earthquake sizes and persistence times for the two phases.

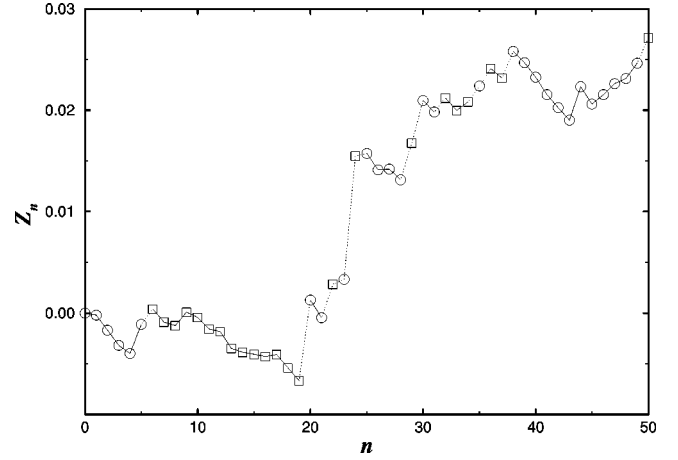


FIG. 3. The process $\{Z_n\}$, which shows the incremental amount of stress needed to keep an earthquake going (see text for the precise definition). Each failure event corresponds to a segment of the process that starts out from a maximum up to that point and ends when it exceeds that level, and is marked as alternating circles and squares. The sample shown here, which corresponds to the stress distribution shown in the inset of Fig. 2(a), depicts events of size 6, 14, 2, 1, 1, The fault is loaded adiabatically between these events, during the intervals when $\{Z_n\}$ moves monotonically up from one maximum to the next. These are shown as dotted lines connecting consecutive events.

A. Gutenberg-Richter phase

Let us first focus on the GR phase. At some instant t immediately preceding a cell failure, consider the sequence $\{X_n \equiv 1 - s_{i(n+1)}\}$, where $i(n)$ is the index of the cell that has the n th largest stress in the system [see Fig. 3]. For a large system, the stress gaps $\{\delta s_n = X_{n-1} - X_n\}$ are (almost) independent of each other, drawn from an exponential probability distribution, i.e., $\text{Prob}(\delta s_n = s) = \exp(-\bar{p}Ns)$, with $\bar{p} \equiv \langle (1 - s_a)^{-1} \rangle$. For $n \gg 1$, X_n resembles a biased random walk with a mean $\mu_X(n) = n/(\bar{p}N)$ and variance $\sigma_X^2(n) = n/(\bar{p}N)^2$. As long as dynamical effects are absent, the stress redistributed to each cell following the failure of the first n cells is given by a random variable Y_n with mean $\mu_Y(n) = nc/(\bar{p}N)$ and variance $\sigma_Y^2(n) \approx n(cW/\bar{p}N)^2 \ll \sigma_X^2(n)$. A triggered earthquake can sustain itself only if the redistributed stresses exceed the stress gaps. Therefore $Z_n \equiv X_n - Y_n < 0$ during an earthquake and it immediately follows that the distribution of earthquake sizes for $N \gg n \gg 1$ is given in terms of the distribution of first passage times of biased random walks. Approximating the continuous probability distribution of the step sizes of $\{Z_n\}$ with a Bernoulli process (where steps of equal size are taken up or down with probability p and $1 - p$, respectively), we can utilize results available for Bernoulli trials [14],

$$\text{Prob}(Z_i < 0, 0 < i < n; Z_n = 0) = \frac{\text{Prob}(Z_n = 0)}{n}, \quad (13)$$

i.e., the probability for the *first* return to the origin after n steps equals the total probability of reaching the origin after n steps divided by n . $\text{Prob}[Z_n = 0]$ can easily be calculated [14] for $N \gg n \gg 1$. One obtains Eq. (6) with $n_{cf} = 2(\mu^2 + \sigma^2)/\mu^2$, where μ and σ^2 are the mean and variance of the

step size for the process Z_n , respectively. Substituting the values $\mu = (1-c)/(\bar{p}N)$ and $\sigma^2 \approx 1/(\bar{p}N)^2$, the cutoff length is given by

$$n_{cf} \approx 2[1 + (1-c)^{-2}] = \frac{2}{(1-c)^2} \{1 + O((1-c)^2)\}, \quad (14)$$

where the last approximation is justified since treating Z_n as a Bernoulli process is expected to yield relative errors of $O(\mu^2/\sigma^2)$.

For finite-sized systems, when the fraction of failed cells $r = n/N$ is no longer small, Eq. (6) needs to be modified since the stress gaps are not entirely independent: In order to correctly reflect the fact that $Z_N = 1 - c$ to within $O(1/N)$, the Bernoulli process should be constrained to return to its mean value after N steps. This can be achieved by calculating the corresponding conditional probabilities:

$$p_e^{(f)}(n) = \frac{\text{Prob}(Z_n = 0) \text{Prob}(Z_{N-n} = 1 - c)}{n \text{Prob}(Z_N = 1 - c)} = \frac{\tilde{A}_f}{n^{3/2}} \exp\left\{-\frac{n(1+n/N)}{n_{cf}}\right\}, \quad (15)$$

which reduces to Eq. (6) in the limit $n \ll N$. (\tilde{A}_f is a constant fixed by normalization.) Figure 2(a) shows the distribution of event sizes for numerical simulations of the model with $N = 400$, for values $c = 0.6, 0.7$, and 0.8 . (In all presented simulation results, $W = 2/19$ and $\epsilon = 0.5$.) The continuous lines are one-parameter fits to the form (15). The discrepancy between the fitted and theoretical [from Eq. (14)] values of n_{cf} is consistent with the expected relative error.

As mentioned earlier, the failure of all the remaining cells becomes very likely once $(1-\epsilon)N/c$ cells have failed, since the initially failed cells reach their dynamical failure stress. The mean event size is roughly equal to $n_{cf}^{1/2}$, therefore the mean time between events is $T_0 n_{cf}^{1/2}/N$, where $T_0 \equiv \langle \tau_{s,i} - \tau_{a,i} \rangle / (K_L v)$ is the characteristic time over which a cell is loaded from its arrest stress to its failure stress. The typical waiting time to see a switch to the runaway phase yields [cf. Eq. (15)]

$$T_{f \rightarrow r} \approx T_0 \frac{C_{fr} N^{1/2}}{n_{cf}^{1/2}} \exp\left\{\frac{(1-\epsilon)(1-\epsilon+c)}{c^2 n_{cf}} N\right\}, \quad (16)$$

with C_{fr} a factor of order unity which varies weakly with ϵ and c in the region of interest, provided that each attempt is statistically independent of each other. We verified that in our simulations indeed no time correlations of event sizes were present, out to many times the characteristic time T_0 (see also the Discussion section). The distribution of persistence times should then obey Poisson statistics with mean $T_{f \rightarrow r}$. Figure 4 depicts the distribution of persistence times (with a fit to Poisson statistics) for $N = 400$ and $c = 0.73$. Mean persistence times depend very sensitively on the conservation parameter c , as shown in the inset of Fig. 4 [15].

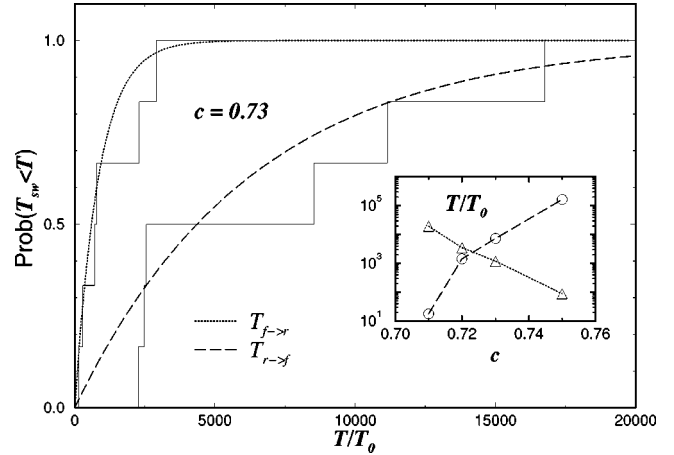


FIG. 4. Distribution of persistence times $T_{f \rightarrow r}$ and $T_{r \rightarrow f}$ for $W = 2/19$, $\epsilon = 0.5$, $N = 100$, $c = 0.73$. The lines are fits of the cumulative probabilities to the Poisson distribution. (Simulations for systems with other parameters that allowed for many more switches during the simulated times clearly also gave Poisson distributions for the distribution of persistence times.) Inset: The dependence of persistence times on conservation parameter c (triangles $T_{f \rightarrow r}$, circles $T_{r \rightarrow f}$) for the same values of W , ϵ , and N . Statistical errors are comparable to symbol sizes.

B. Runaway phase

Let us next consider the runaway phase. Immediately preceding the first cell failure after a runaway event, the stress gaps $\{\delta s_n = X_{n-1} - X_n\}$ have the probability distribution $\text{Prob}(\delta s_n = s) = \exp[-\bar{p}Ns/(1-\epsilon)]$. Hence, $\{X_n\}$ has a mean $\mu_X(n) = n(1-\epsilon)/(\bar{p}N)$ and variance $\sigma_X^2(n) = n(1-\epsilon)^2/(\bar{p}N)^2$. As long as dynamical effects are absent, the stress redistributed to each cell following the failure of the first n cells is still given by $\{Y_n\}$ with mean $\mu_Y(n) = nc/(\bar{p}N)$ and variance $\sigma_Y^2(n) \approx n(cW/\bar{p}N)^2 \ll \sigma_X^2(n)$. Thus the mean and variance of the step size for $\{Z_n\}$ are $\mu = (1-\epsilon-c)/(\bar{p}N)$ and $\sigma^2 \approx (1-\epsilon)^2/(\bar{p}N)^2$. The probability for an earthquake to terminate after n cell failures is [including finite-size corrections in analogy with Eq. (15)]

$$p_e^{(r)}(n) \approx \frac{\tilde{A}_r}{n^{3/2}} \exp\left\{-\frac{n(1+n/N)}{n_{cr}}\right\}, \quad (17)$$

$$n_{cr} = \frac{2(1-\epsilon)^2}{[c - (1-\epsilon)]^2} \{1 + O[(c - (1-\epsilon))^2]\}, \quad c > 1 - \epsilon. \quad (18)$$

Since $\mu < 0$ for $1 - \epsilon < c$, $Z_n < 0$ with finite probability for all n and a runaway event occurs. In fact, a runaway event is inevitable since $Z_N < 0$ and the runaway event will commence once $\{Z_n\}$ reaches its maximum. The total number of cells that fail before a runaway event is given by the position of the maximum of $\{Z_n\}$, whose probability distribution is proportional to $n_{cr} p_e^{(r)}(n)$ for $n \gg n_{cr}$. The mean number of these ‘precursor’ cells is of order $n_{cr}^{1/2}$, which remains a finite constant as $N \rightarrow \infty$, i.e., for big systems almost all the slip happens during the runaway events [16].

The remaining cells will all fail during the runaway event. Imagine a situation where a fraction $r > (1 - \epsilon)/c$ of the cells have failed. At that point, the total redistributed stress per cell is

$$\begin{aligned} S &= c \left[r + \left(r - \frac{1 - \epsilon}{c} \right) \{ c + c^2 + \dots \} \right] \\ &= \frac{c[r - (1 - \epsilon)]}{1 - c}, \end{aligned} \quad (19)$$

where the second term arises from repeat failures of some cells. $S \geq 1$ is needed to ensure that small event cells fail again and recreate the stress distribution (10). This is achieved if

$$r \geq r^* \equiv \frac{1}{c} - \epsilon.$$

Thus the large event cannot recreate the stress distribution (10) if more than $(1 - r^*)N = r_c N$ cells fail during background activity. This usually leads to a breakup of the bunched stress distribution and subsequent evolution towards the GR stress distribution (8). The typical persistence time of the runaway phase before a switch to the GR phase is [15]

$$\begin{aligned} T_{r \rightarrow f} &\approx T_0 \frac{C_{rf} N^{3/2}}{n_{cr}^2} \\ &\times \exp \left[\frac{(c - c^*) [1 + (c - c^*) / (c^* c)] N}{c^* c n_{cr}} \right], \\ c &> c^* \end{aligned} \quad (20)$$

provided that all attempts are statistically independent of each other. (We have explicitly checked in the simulations that in the runaway phase, the particular realizations of stress distributions immediately following a large event are statistically independent of each other [17]). $T_{r \rightarrow f}$ becomes comparable to the typical time between runaway events when $c \searrow c^*$, as expected [18]. Figure 4 depicts the distribution of persistence times and a fit to Poisson statistics for $N = 100$ and $c = 0.73$. The inset shows the dependence of mean persistence times on c for $N = 100$. Although agreement with Eqs. (16) and (20) is rather poor, the strong exponential dependence as a function of conservation parameter is evident.

IV. DISCUSSION

The persistence times in both the GR phase and the runaway phase diverge exponentially with system size for $(1 + \epsilon)^{-1} < c < 1$, and the system remains in either phase for extremely long times, thus the phase space has two almost stable attractors. Clearly, the runaway phase represents a more ‘‘ordered’’ stress distribution. Indeed, the basin of attraction for the runaway phase is extremely small. In order to quantify this aspect, consider the ‘‘configurational entropy’’ for a given stress distribution $p(\tilde{s})$, with $\tilde{s}_i \equiv (\tau_i - \tau_{a,i}) / (\tau_{f,i} - \tau_{a,i})$:

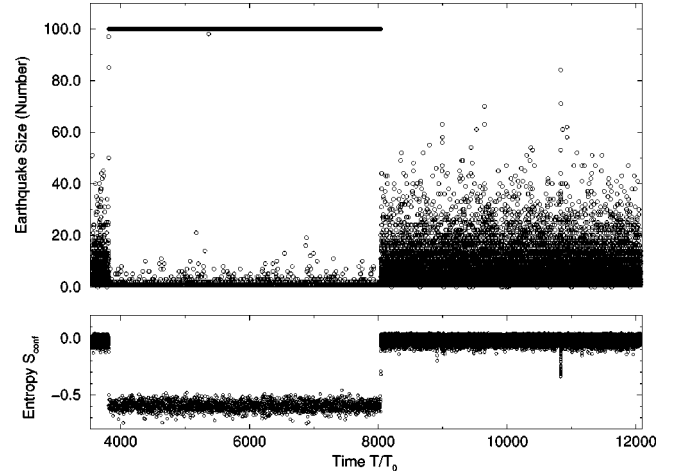


FIG. 5. Sample time series of earthquake sizes (top), plotted together with the conformational entropy $S_{\text{conf}}(t)$ (bottom) for $W = 2/19$, $\epsilon = 0.5$, $N = 100$, $c = 0.73$. [For the calculation of $S_{\text{conf}}(t)$, the simulated stress distribution was approximated by a ten bin histogram of the stress values, which was evaluated immediately after each earthquake.] The earthquake size distribution changes drastically every time S_{conf} toggles from 0 to $\ln(1 - \epsilon)$, indicating a transition from one phase to the other. A failed switching attempt from the GR phase to the runaway phase is seen at about $T/T_0 = 10\,900$.

$$S_{\text{conf}}(\{p\}) \equiv - \int d\tilde{s} p(\tilde{s}) \ln[p(\tilde{s})]. \quad (21)$$

For the GR phase, $S_{\text{conf}}^{(f)} = 0$, indicating that a ‘‘generic’’ stress distribution characterizes the GR phase. On the other hand, in the runaway phase

$$S_{\text{conf}}^{(r)} = - \int d\tilde{s} p^{(r)}(\tilde{s}) \ln[p^{(r)}(\tilde{s})] = \ln(1 - \epsilon), \quad (22)$$

indicating that the stress distribution is highly organized in that phase. For discrete N the stress distribution is approximated by a histogram of the stress values, and the integral is replaced by the sum over all bins of the histogram.

The time evolution of the configurational entropy of the stress distribution, calculated with a ten bin histogram, is depicted in Fig. 5 along with event sizes. It is clear that $S_{\text{conf}}(t)$ can be used as an ‘‘order parameter,’’ a number that distinguishes the GR phase and the runaway phase, with the advantage that it can be determined at any instant. Histograms of event sizes require a finite time interval to collect, and there is always the danger of mixing events from one phase with the other, thereby confusing the picture: The cumulative event size distribution over many persistence times is a weighted average of two entirely different event distributions, which obscures the underlying physical phenomena. S_{conf} provides a reliable way to separate the two phases and makes it possible to accumulate accurate event size distributions for both of them. Unfortunately, such a quantity cannot be determined from existing field data since the spatial distribution of stress is unknown.

So far, the discussion has centered around the $W \ll 1$ limit, and the main role played by the heterogeneities has been the ‘‘randomization’’ of the stress distribution at time scales

over which all cells fail a few times. The distribution of loading times, over which the cells are loaded from the individual arrest stress to the failure stress, has a mean $T_0 \equiv \langle \tau_{s,i} - \tau_{a,i} \rangle / (K_1 \nu)$ and standard deviation of order WT_0 . Therefore the “randomization” time, over which the stress variables s_i become roughly uncorrelated, is of order T_0/W . Thus, even for small W , for large enough N this will be small compared to the persistence times, which scale exponentially in N [see Eqs. (16) and (20)]. This ensures the consistency of the assumption that the earthquakes are basically statistically independent of each other. The validity of this assumption of statistical independence can be explicitly verified by examining the time correlations of event sizes numerically; indeed no trace of any correlation was found in our simulations, out to many times the randomization time T_0/W . Likewise, we have explicitly checked that in the runaway phase, the particular realizations of stress distributions immediately following a large event are statistically independent of each other [17].

For finite values of $W < 2$, we expect most of the features to remain qualitatively unchanged: In the GR phase, the exponential cutoff size still diverges as $n_{cf} \sim (1-c)^{-2}$, and although c^* in general depends on W and the shape of $\rho(s_a)$, there is still a persistent runaway phase for $c^* < c \leq 1$. However, the situation is likely to change qualitatively once arrest stresses can be arbitrarily close to failure stresses, i.e., $W=2$, and new values for the arrest stresses are picked every time a cell fails [19]. This corresponds to the situation discussed in Ref. [4] for finite-dimensional systems. Immediately upon introduction of dynamical weakening ($\epsilon > 0$), $n_{cf} \sim \epsilon^{-2}$ when c approaches 1, i.e., the cutoff size no longer diverges. Furthermore, for $c=1$ the GR phase is no longer persistent since the persistence time $T_{f \rightarrow r}$ remains finite for large N .

Some of the results presented for the mean-field model, especially the qualitative phase diagram, calculated exponents for the power-law earthquake distributions, and the divergence of the cutoff length scale, can be expected to apply to models with realistic interactions, up to logarithmic corrections. This is because the underlying critical points that control these exponents remain mean-field-like down to two-dimensional (2D) faults. This result is firmly established for the $\epsilon=0$ case [4,6]. At finite ϵ one expects the nucleation size for the runaway phase, which equals $(1-\epsilon)N/c$ in mean-field theory, to become independent of the system size, since elastic forces in the fault plane concentrate stresses along the earthquake rupture front as the earthquake progresses. Earthquakes bigger than a finite nucleation size N_{crack} become unstoppable in the presence of dynamic weakening effects and small disorder [3], and rupture the entire fault. Nevertheless, for $n_{cf} < N_{\text{crack}}$, the mean-field scaling results may still apply at finite ϵ , provided that $W < 2$, i.e., there is a finite minimum stress drop associated with each cell failure. For systems with $N_{\text{crack}} > N$, this range will extend all the way to the fault size. In this case, one remarkable consequence is that since generically $(1-c) \sim 1/\sqrt{N}$ [4,5], the cutoff size in the GR phase $n_{cf} \sim (1-c)^{-2} \sim N$, i.e., earthquakes on individual fault zones obey power-law statistics for events up to a finite fraction of the entire system size.

In this paper we have implicitly assumed that all earthquakes are effectively two dimensional, even though the

brittle seismogenic zone has a finite width. Our assumption is justified by observations and the context of the model (size of assumed fault). In general, earthquakes with magnitude about M6.3 break the entire seismogenic zone. Up to this size it is accepted that events are roughly two dimensional. When the aspect ratio of the rupture dimensions width/length is much less than 1 the event is expected intuitively to become more 1D-like. For very large earthquakes a corresponding change in the slope of earthquake statistics was predicted [20] and claimed to have been observed [21]. This, however, is controversial. Kagan [22] has argued that those inferences are not supported by a more robust analysis. Thus there is no conclusive evidence that the dimensionality changes from 2D to 1D at a certain event size. The lack of a clearly observed transition in the available data suggests that events penetrate deeper than the width of the seismogenic zone, into the underlying viscoelastic substrate, and continue to grow in width as they increase in length. Also, in our simulations [4] of a two-dimensional fault with length and width of computational grid 70 and 17.5 km, embedded in a three-dimensional elastic half space, the largest events are about M6.5. The aspect ratio of those rupture areas is not very different from 1, so in the quasistatic limit we expect mean-field theory to apply roughly up to the largest events. This is confirmed by comparing the corresponding simulation results with mean-field theory predictions [4].

An important result is the possibility that a fault system might switch spontaneously from a “Gutenberg-Richter” earthquake distribution to a “characteristic” earthquake distribution, as in the mean-field model. We note that calculations based on an entirely different model, simulating the coupled evolution of regional earthquakes and faults in a rheologically layered 3D solid [10], show similar behavior. Clear observation of such mode switching in nature requires data sets spanning many thousands of years. Paleoseismic studies attempt to construct long histories of seismic events at given locations from sequences of displaced and highly disturbed rock layers. Remarkably, the longest available paleoseismic records, documenting large earthquake activity along the Dead Sea transform in Israel [7], appear to be characterized by alternating phases of intense seismic activity lasting a few thousands of years, and periods of comparable length without large seismic events. Other, qualitatively similar alternating deformation phases have been documented in the eastern California shear zone [8] and the Great Basin Province in the western U.S. [9].

Another intriguing possibility might arise in a fault system of weakly coupled segments driven under similar conditions. The seismic response of such systems might exhibit a sort of “coexistence,” i.e., a fraction of the patches might follow characteristic scaling whereas the others obey Gutenberg-Richter scaling, giving rise to a hybrid event size distribution. This may explain examples in the data of Ref. [2], where the characteristic “bump” in the distribution was not very pronounced. Finally, we note that part or all of the low magnitude seismicity in the GR phase may be too small to be detected by a seismic network. In this case the spontaneous switching between the runaway and GR phases may be interpreted as transitions from seismic response of a fault system to creeplike behavior.

ACKNOWLEDGMENTS

We have greatly benefited from extensive discussions with Daniel S. Fisher, Jim Rice, and Sharad Ramanathan. K.D. gratefully acknowledges support from the Society of Fellows of Harvard University, and the NSF via Grant Nos. DMR 9106237 and 9630064, Harvard's MRSEC, and Har-

vard's Milton Fund. D.E. acknowledges support by the NSF through Grant Nos. DMR-9106237, DMR-9417047, and DMR-9416910. Y.B.Z. was supported by the Southern California Earthquake Center (based on NSF Cooperative Agreement No. EAR-8920136 and USFS Cooperative Agreement No. 14-08-0001-A0899).

-
- [1] B. Gutenberg and C. F. Richter, *Ann. Geofis.* **9**, 1 (1956). The development and dynamics of fault systems has been studied as a nonequilibrium critical phenomenon by, e.g., K. Chen, P. Bak, and S. P. Obukhov, *Phys. Rev. A* **43**, 625 (1991); P. Miltenberger, D. Sornette, and C. Vanneste, *Phys. Rev. Lett.* **71**, 3604 (1993); P. A. Couie, C. Vanneste, and D. Sornette, *J. Geophys. Res.* **98**, 21809 (1993).
- [2] S. G. Wesnousky, *Bull. Seismol. Soc. Am.* **84**, 1940 (1994); M. W. Stirling, S. G. Wesnousky, and K. Shimazaki, *Geophys. J. Int.* **123**, 833 (1996).
- [3] Y. Ben-Zion and J. R. Rice, *J. Geophys. Res.* **98**, 14 109 (1993); **100**, 12 959 (1995); Y. Ben-Zion, *ibid.* **101**, 5677 (1996).
- [4] D. S. Fisher, K. Dahmen, S. Ramanathan, and Y. Ben-Zion, *Phys. Rev. Lett.* **78**, 4885 (1997).
- [5] K. Chen, P. Bak, and S. P. Obukhov, *Phys. Rev. A* **43**, 625 (1991).
- [6] D. Ertas and M. Kardar, *Phys. Rev. E* **49**, R2532 (1994).
- [7] S. Marco, M. Stein, A. Agnon, and H. Ron, *J. Geophys. Res.* **101**, 6179 (1996).
- [8] T. Rockwell (private communication).
- [9] R. E. Wallace, *Bull. Seismol. Soc. Am.* **77**, 868 (1987).
- [10] Y. Ben-Zion, V. Lyakhovskiy, and A. Agnon, *EOS Trans. Am. Geophys. Union* **79**, S222 (1998); V. Lyakhovskiy, Y. Ben-Zion, and A. Agnon (unpublished).
- [11] R. Burridge and L. Knoppoff, *Bull. Seismol. Soc. Am.* **57**, 341 (1967); J. M. Carlson, J. S. Langer, and B. E. Shaw, *Rev. Mod. Phys.* **66**, 658 (1994), and references therein; C. R. Myers, B. E. Shaw, and J. S. Langer, *Phys. Rev. Lett.* **77**, 972 (1996); J. B. Rundle, W. Klein, and S. Gross, *ibid.* **76**, 4285 (1996); D. Cule and T. Hwa, *ibid.* **77**, 278 (1996).
- [12] K. Christensen and Z. Olami, *Phys. Rev. A* **46**, 1829 (1992), and references therein.
- [13] Note that cell stresses do not necessarily get arrested at $\tau_{a,i}$ during an earthquake, which would have required the slip amount to be $(\tau_i - \tau_{a,i})/(K_L + J)$ instead. We use Eqs. (2) in order to mimic continuous time. This choice also makes the model Abelian, i.e., whether a given cell will fail during an earthquake does not depend on which order they fail, simplifying the analysis.
- [14] W. Feller, *An Introduction to Probability Theory and Its Applications*, 2nd ed. (John Wiley & Sons, Inc., New York, 1957), Vol. 1, Chap. XI.
- [15] The estimate for the persistence time does not take into account possible two or many step channels to nucleate from one phase into the other. Such corrections, however, are not expected to change the exponential dependence of the persistence time on the system size, i.e., the metastability of the two phases in the considered parameter regime.
- [16] For larger disorder W there are yet another kind of background events. Their number is proportional to N . In the regime considered here (small W , and moderate N), however, those effects are negligible, as is also confirmed by our simulation results.
- [17] One exception to the statistical independence of events happens during the breakup of the runaway stress distribution, where atypically large (for the GR phase) earthquakes occur within a few T_0 of the initiation of breakup. These events should not be included in an analysis of the event size distributions, since they are simply transients and not representative of events in steady state.
- [18] Note that n_{cr} remains finite when $c \searrow c^*$, therefore the cutoff size for background small events never diverges; the underlying "critical point" is obscured by the breakup instability.
- [19] The nature of the heterogeneities in our model differs significantly from those considered in Ref. [4], in that they are *long range* in the displacements u , although short range in position. This is the physically relevant situation when typical slips of a cell are smaller than the linear cell size, so that substantially, the same portions of the the two plates face each other before and after a slip. In Ref. [10], the heterogeneities evolve as a function of the deformation in a damage rheology model.
- [20] J.B. Rundle, *J. Geophys. Res.* **94**, 12337 (1989).
- [21] J. F. Pacheco, C. H. Scholz, and L. R. Sykes, *Nature (London)* **255**, 71 (1992).
- [22] Y. Y. Kagan, *Physica D* **77**, 160 (1994).